

Outer Retinal Structure in Patients With Acute Zonal Occult Outer Retinopathy

MARIANNA MKRTCHYAN, BRANDON J. LUJAN, DAVID MERINO, CHARLES E. THIRKILL, AUSTIN ROORDA, AND JACQUE L. DUNCAN

• **PURPOSE:** To correlate visual function with high-resolution images of retinal structure using adaptive optics scanning laser ophthalmoscopy (AOSLO) in 4 patients with acute zonal occult outer retinopathy (AZOOR).

• **DESIGN:** Observational case series.

• **METHODS:** Four women, aged 18 to 51, with acute focal loss of visual field or visual acuity, photopsia, and minimal fundus changes were studied with best-corrected visual acuity (BCVA), Goldmann kinetic and automated perimetry and fundus-guided microperimetry, full-field and multifocal electroretinography (ffERG and mfERG), spectral-domain optical coherence tomography (SD-OCT), and AOSLO imaging. Cone spacing was measured in 4 eyes and compared with 27 age-similar normal eyes. Additional functional testing in 1 patient suggested that cones were absent but rods remained. Serum from all patients was analyzed for anti-retinal antibody activity.

• **RESULTS:** In all patients vision loss was initially progressive, then stable. Symptoms were unilateral in 2 and bilateral but asymmetric in 2 patients. In each patient, loss of retinal function correlated with structural changes in the outer retina. AOSLO showed focal cone loss in most patients, although in 1 patient with central vision loss such change was absent. In another patient, structural and functional analyses suggested that cones had degenerated but rods remained. Anti-retinal antibody activity against a ~45 kd antigen was detected in 1 of the patients; the other 3 patients showed no evidence of abnormal anti-retinal antibodies.

• **CONCLUSIONS:** Focal abnormalities of retinal structure correlated with vision loss in patients with AZOOR. High-resolution imaging can localize and demonstrate the extent of outer retinal abnormality in AZOOR patients. (*Am J Ophthalmol* 2012;153:757-768. © 2012 by Elsevier Inc. All rights reserved.)

Accepted for publication Sept 1, 2011.

From the School of Optometry, University of California Berkeley, Berkeley, California (M.M., B.J.L., A.R.); Department of Ophthalmology, University of California San Francisco, San Francisco, California (D.M., J.L.D.); and Ocular Immunology Laboratory, University of California Davis, Davis, California (C.E.T.).

Inquiries to Jacque L. Duncan, Department of Ophthalmology, University of California, San Francisco, 10 Koret Way, #K129, San Francisco, CA 94143-0730; e-mail: DuncanJ@vision.ucsf.edu

ACU TE ZONAL OCCULT OUTER RETINOPATHY (AZOOR) is a syndrome characterized by acute loss of 1 or more zones of visual function, usually accompanied by photopsia, reduced outer retinal function measured by electroretinography in 1 or both eyes, and, in some cases, death of retinal photoreceptor cells without biomicroscopic or fluorescein angiographic abnormalities.¹⁻³ AZOOR occurs more frequently in young myopic women, and recovery of visual function occurs infrequently.¹

The etiology of AZOOR is unknown, but infectious and autoimmune mechanisms have been proposed. Viral or other infectious agents may enter the eye at the optic nerve head or ora serrata and trigger an immune response to viral antigens that are similar to antigens expressed by photoreceptor cells, producing zones of acute photoreceptor cell dysfunction or loss.¹ However, no abnormal anti-retinal antibodies have previously been identified in patients with AZOOR.² Alternatively, genetic factors may predispose some individuals to autoimmune or inflammatory responses against retinal cells, and visual symptoms may develop upon exposure to specific environmental triggers.⁴

Photoreceptor dysfunction is responsible for vision loss in AZOOR, and interocular asymmetry in electroretinographic responses is common. Photoreceptor outer segment dysfunction and degeneration has been correlated with loss or attenuation of the photoreceptor inner segment/outer segment (IS/OS) junction and inner nuclear and outer nuclear layers in regions with visual field defects imaged using time-domain⁵ and spectral-domain optical coherence tomography (SD-OCT) in patients with AZOOR.⁶⁻⁸

Adaptive optics is a set of techniques to reduce blur caused by imperfections in the eye's optics and, when used in an ophthalmoscope, allows for direct imaging of the cone photoreceptor mosaic in vivo.^{9,10} Several reports have demonstrated the utility of using adaptive optics to characterize patients with retinal disease.¹¹⁻¹⁸ In the present article, adaptive optics scanning laser ophthalmoscopy (AOSLO) combined with SD-OCT demonstrated changes in retinal structure that correlated with reduced visual function in 4 AZOOR patients in whom retinal changes sufficient to explain the visual abnormalities were not visible using standard clinical techniques.

TABLE. Summary of Clinical Studies in 4 AZOOR Patients

	Best-Corrected Visual Acuity	ffERG	mfERG	Microperimetry	HVF	SD-OCT	AOSLO	Antibody Against ~45 kd Antigen
Case 1	OD: 20/20 OS: 20/20	Normal amplitude and timing OU, no significant interocular asymmetry	Reduced response densities and delayed timing in the region of scotoma OU	Not performed	Paracentral scotoma OU with normal foveal sensitivities (37 dB OD, 38 dB OS)	Disrupted IS/OS junction OU in regions of reduced cone reflectivity	Reduced cone reflectivity in the region of scotoma OD	Not detected
Case 2	OD: 20/20 OS: 20/20-1	20% decrease in photopic and scotopic amplitudes OS compared to OD	Reduced response densities and delayed timing in the region of scotoma OS	Cone-mediated scotoma with rod-mediated sensitivity in the region of scotoma OS	Paracentral scotoma with normal foveal sensitivity (40 dB) OS	Reduced reflectance of IS/OS junction within scotoma region OS	Absence of cones in the region of scotoma OS with higher-density cells suspected to be rods	Not detected
Case 3	OD: 20/200+1 OS: 20/20	Reduced photopic b-wave amplitude by 33% OD relative to OS and reduced 30 Hz flicker implicit time (30 ms OD vs 27.5 ms OS)	Reduced response densities and delayed timing centrally OD	Severe loss of foveal sensitivity by 3.5 log units OD	Temporal scotoma extending into fixation OD	Relative thinning of outer nuclear layer and ganglion cell layer, intact ELM-OS/RPE in the region of scotoma OD compared with OS	Normal cone mosaic in the region of reduced foveal sensitivity OD	Not detected
Case 4	OD: 20/200 OS: 20/200	Normal amplitude and timing OU, 20%-25% lower response to all stimuli OD compared to OS	Reduced response densities and delayed timing centrally OU	Reduced sensitivity in the fovea OU	Central scotoma OU with reduced foveal sensitivities (18 dB OD, 26 dB OS)	Loss of IS/OS junction in the central macula with thinning of outer nuclear layer OU	Abnormal cone coverage and spacing within macula OD	Detected

AOSLO = adaptive optics scanning laser ophthalmoscopy; ELM = external limiting membrane; ffERG = full-field electroretinography; HVF = Humphrey visual field; IS/OS = inner segment/outer segment; mfERG = multifocal electroretinography; RPE = retinal pigment epithelium; SD-OCT = spectral-domain optical coherence tomography.

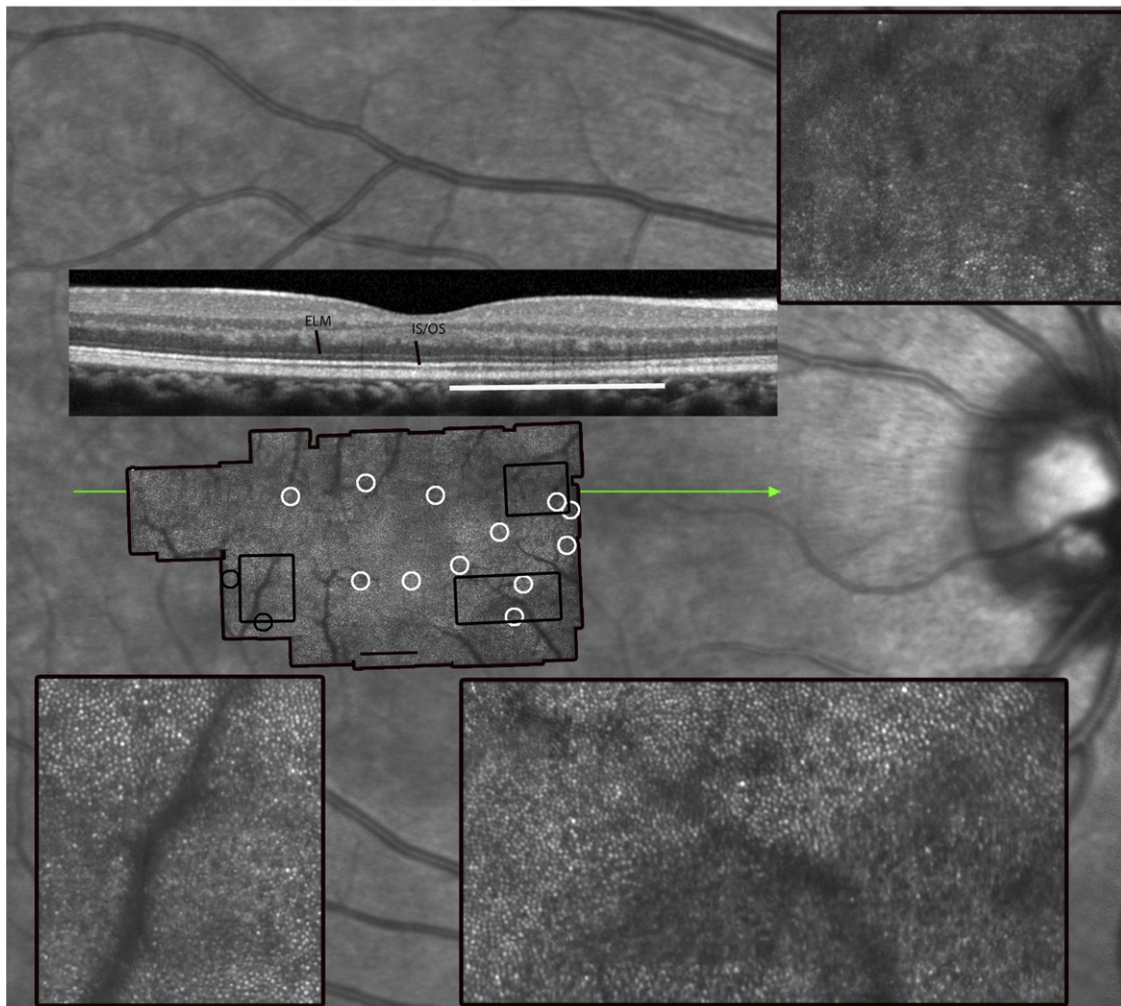
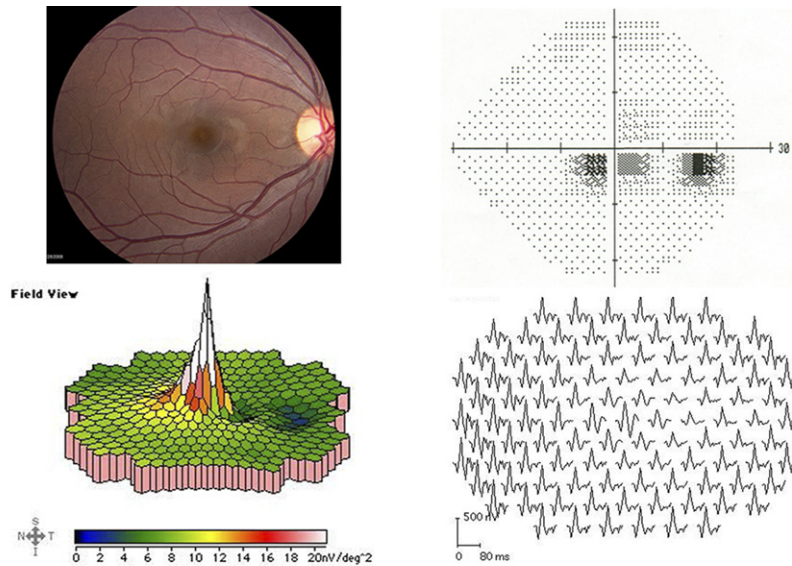


FIGURE 1. Acute zonal occult outer retinopathy, Patient 1, right eye. Similar findings were present in the left eye (not shown). (Top left) The fundus examination was normal. (Top right) Parafoveal visual field (VF) defects with normal foveal sensitivities. (Middle) The multifocal electroretinographic first-order response traces, displayed in field view, reveal a discrete region, 5 degrees temporal to fixation, of abnormally reduced response densities with delayed timing. (Bottom) Adaptive optics scanning laser ophthalmoscopy (AOSLO) images superimposed on an infrared fundus image reveal abnormal cone reflectivity in regions corresponding to the visual field defects and reduced multifocal electroretinography (mfERG) responses. The composite AOSLO

METHODS

• **COMMON TESTS FOR ALL PATIENTS:** All subjects underwent a complete eye examination including best-corrected visual acuity measured according to the Early Treatment of Diabetic Retinopathy Study protocol, slit-lamp biomicroscopy, color fundus photography, and infrared fundus photography with SD-OCT (Spectralis HRA + OCT Laser Scanning Camera System; Heidelberg Engineering, Vista, California, USA). Goldmann kinetic perimetry was performed with I3c, V3c, and I4e targets, and automated perimetry was completed with measurement of foveal thresholds using a Goldmann III stimulus on a white background (31.5 asb) and exposure duration of 200 ms; patients were tested using either the 30-2, 24-2, or 10-2 protocol depending on the extent and location of the scotoma (SITA Standard, Humphrey Visual Field Analyzer; HFA II 750-6116-12.6; Carl Zeiss Meditec, Inc, Dublin, California, USA). Pupils were dilated with 1% tropicamide and 2.5% phenylephrine before bilateral full-field electroretinography (ffERG) was performed after 45 minutes of dark adaptation using Burian-Allen contact lens electrodes (Hansen Ophthalmic Development Laboratory, Iowa City, Iowa, USA), as described previously.¹⁶ Eyes were tested simultaneously and measured individually, according to standards specified by the International Society for Clinical Electrophysiology and Vision (ISCEV).¹⁹ Multifocal ERG (mfERG) testing was performed in a light-adapted state (VERIS 5.1.10C, Electrodiagnostic Imaging, Inc, Redwood City, California, USA) with Burian-Allen contact lens electrodes, also according to ISCEV standards²⁰ and as described previously.¹⁶ Fundus-guided microperimetry (MP-1; Nidek Technologies America Inc, Greensboro, North Carolina, USA) used a Goldmann size III stimulus of 200 ms duration with a 4-2 threshold strategy as described previously.¹⁶ Serum from all patients was analyzed for anti-retinal antibody activity using Western blots of porcine retina (PelFreez, Rogers, Arkansas, USA) at the Ocular Immunology Laboratory, UC Davis, California. Magnetic resonance imaging (MRI) of the brain and orbits with and without contrast was performed in Patients 2 and 3 to exclude central nervous system or orbital disease.

• **ASSESSMENT OF ROD- AND CONE-MEDIATED SENSITIVITY:** In Patient 2, 2-color dark-adapted Goldmann perimetry and fundus-guided 2-color dark-adapted microperimetry were used to investigate localized rod and cone function. Chromatic dark-adapted 2-color kinetic perimetry was performed to measure the rod contribution to the dark-adapted kinetic visual field.²¹ In order to ensure that the parameters were correct for measuring rods, fields were measured and sensitivity was compared for 2 different wavelengths.²¹ Visual fields were measured for the Goldmann I3c and V3c target sizes, each with a long-wavelength and a short-wavelength filter, as described previously.²¹ The long-wavelength filter had a cut-on at 600 nm, while the short-wavelength filter had a cutoff at 510 nm. Long-wavelength and short-wavelength filters used were Wratten 25 and 47B, respectively. The stimuli were 2 log units lower in luminance (I3c and V3c) for the short-wavelength stimulus, based on the spectral emittance of the Goldmann perimeter bulb, the scotopic luminance efficiency function, and spectral transmittance of the chromatic filters.²¹ A fixation target was provided with a dim red light presented in the Ganzfeld dome. The background light in the bowl was occluded by moving the sliding diaphragm up to its maximal height, in addition to covering it with several layers of blackout cloth to prevent any light leakage. To monitor the patient's fixation, monovision night goggles (Zenit NV, Famous Trails, San Diego, California, USA) were employed. Two healthy normal subjects were also tested to verify that the stimuli were matched scotopically.

Two-color dark-adapted microperimetry was also performed to investigate retinal sensitivity with higher resolution using a custom test pattern with a 40-degree testing array using a Goldmann size V stimulus of 200 ms duration spaced in 0.5-degree increments, extending 10 degrees from the fovea in the nasal and temporal directions. Blue (NT30-635, 500 nm short pass) and red (NT30-34, 600 nm long pass; Edmund Industrial Optics, Inc, Barrington, New Jersey, USA) filters were introduced into the stimulus light path with the background set to red, such that the background illumination was effectively 0 cd/m² (Crossland MD, et al. IOVS 2010;51:ARVO E-Abstract 3640). Neutral-density (ND) filters attenuated the red stimulus by 1.0 log unit (NT48-095, Edmund Industrial Optics, Inc)

image, which spans approximately 7.7 × 4.6 degrees, shows areas of reduced cone reflectivity around the foveal center, but otherwise contiguous cones with normal spacing (white circles). The insets, indicated by the black rectangles on the AOSLO montage, highlight retinal regions with contiguous cone coverage interspersed with areas of reduced retinal reflectivity. The lower insets show distinct transitions between normally reflecting cones and reduced reflectance regions with less obvious cone mosaics. The left inset with black circles surrounding it demonstrates a retinal region with abnormal cone spacing. The spectral-domain optical coherence tomography (SD-OCT) scan (green line indicates scan location) shows irregularities in the inner segment/outer segment (IS/OS) junction corresponding with reduced reflectivity of cones. External limiting membrane (ELM) and IS/OS junction layers are labeled. The most affected region of the B-scan is indicated by the white line. Areas of reduced cone reflectivity correspond to regions of reduced sensitivity on the visual field test. Scale bar is 1 degree.

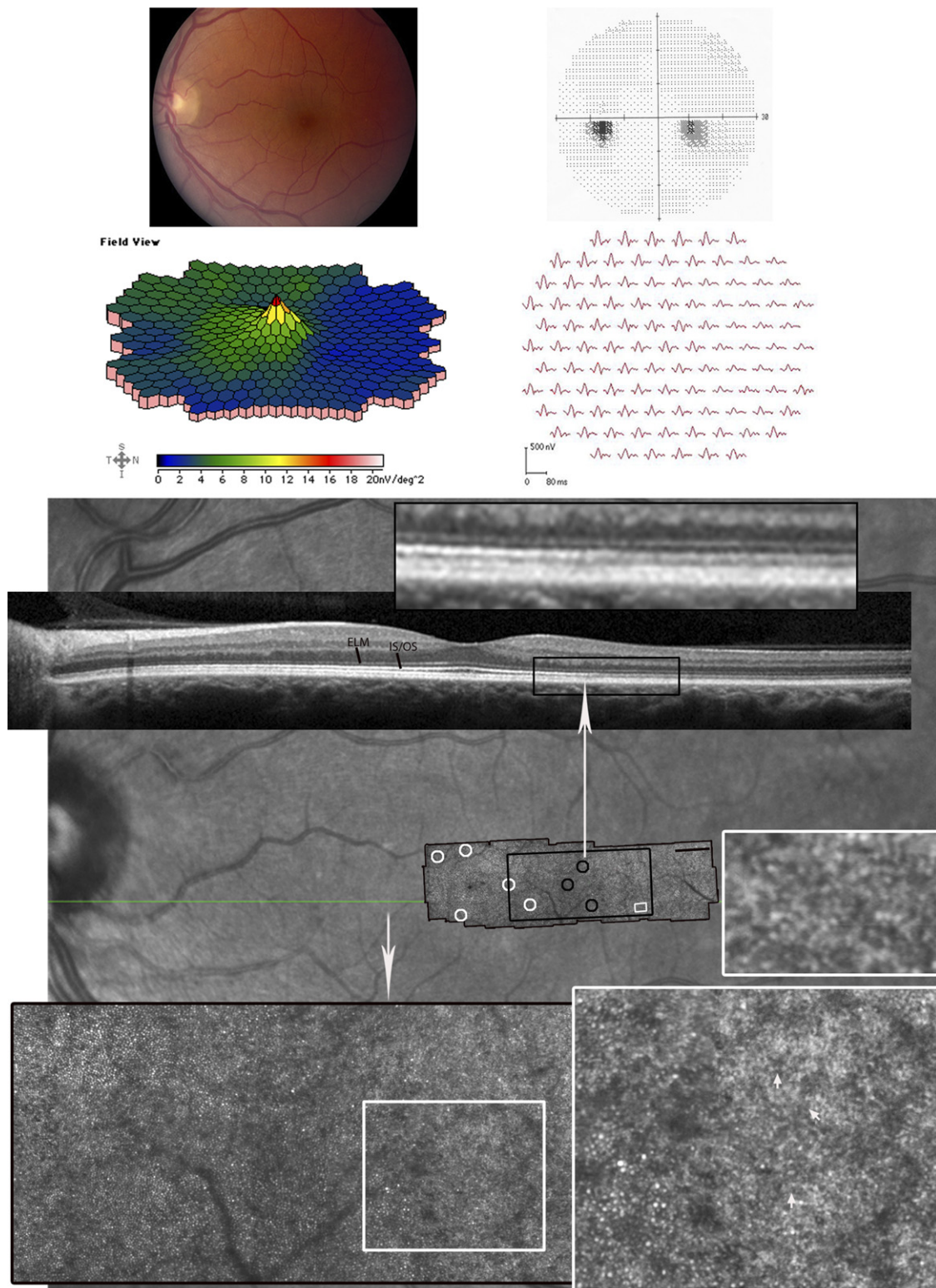


FIGURE 2. Acute zonal occult outer retinopathy, Patient 2, left eye. (Top left) Mild retinal pigment epithelium (RPE) hypopigmentation was present temporal to the fovea. (Top right) Paracentral 10-degree scotoma nasal to fixation with normal foveal sensitivity. (Middle) The multifocal electroretinographic first-order response traces, displayed in field view, reveal a discrete area of reduced response density with delayed timing from 5 to 20 degrees nasal to fixation. The area of reduced function corresponds to the paracentral scotoma present on VF testing and the retinal region with affected cone spacing. (Bottom) The AOSLO image, which spans approximately 8.9×2.4 degrees, is superimposed on an infrared fundus image (scale bar is 1 degree). Cone spacing and coverage are normal (white circles) in all areas except locations near the relative scotoma (demarcated by the long white arrow),

and the blue stimulus by 2.0 log units (NT48-097). After 30 minutes of dark adaptation, rod function was tested using the blue and 2.0 ND filters, then using the red and 1.0 ND filters. Stray light was shielded by placing a black curtain between the patient and the monitor. The patient's fixation was monitored and the chin position was adjusted to maintain good fundus tracking. The sensitivity values for each location using blue dark-adapted (Blue DA) and red dark-adapted (Red DA) stimuli were compared with the expectation that, if the eye was normal, it would show at least 18 dB greater sensitivity to short-wavelength compared to long-wavelength stimuli in the dark-adapted state.²² Given our testing parameters, sensitivity at retinal locations with at least 8 dB greater sensitivity to Blue DA than to Red DA stimuli indicates rod-mediated function, while sensitivities with differences of less than 8 dB indicate cone-mediated function.²³

• **HIGH-RESOLUTION IMAGING:** AOSLO was used to generate high-resolution en-face images of the central retina of the affected eye of each patient, or the better eye in bilateral cases, as described previously.¹⁶ Cone spacing was measured²⁴ at locations in which unambiguous cones were visualized, and compared to normative data from 27 age-similar individuals.¹⁶ Cone spacing greater than 2 standard deviations above the normal mean at that location was considered abnormal.^{13,14,16}

RESULTS

THE TABLE PROVIDES A SUMMARY OF CLINICAL RESULTS for all 4 patients.

• **CASE 1:** An 18-year-old healthy emmetropic woman presented 5 weeks after the acute onset of scotomas and photopsias in both eyes. Past medical history included migraines and seasonal allergies, with no history of autoimmune disease. There were no fundus abnormalities in either eye (Figure 1; right eye shown). Multifocal ERG revealed localized macular outer retinal dysfunction.

AOSLO images within the foveal center showed normal cone spacing and density.¹⁶ Beyond 1.5 degrees, cone reflectivity was reduced, but cone spacing was normal and contiguous except in a region adjacent to a patch of weakly reflecting retina (Figure 1). The patient experienced no improvement or progression of visual loss, and repeated

perimetry, mfERG, AOSLO, and SD-OCT studies showed no significant changes over 14 months.

• **CASE 2:** A 42-year-old myopic woman presented with acute onset of a blind spot in her left eye associated with transient flashing lights that occurred only in total darkness. The patient had a history of complex partial seizures, hypertension, panic disorder, psychogenic amnesia, and short-term memory loss. MRI of the head with and without contrast was normal.

AOSLO imaged the transition from normal cone spacing and coverage¹⁶ to a region beginning 4 degrees temporal to the fovea corresponding to a discrete scotoma where cones were less contiguous and showed increased spacing^{13,14,16} (Figure 2). Beyond 4 degrees, regularly arranged cells were observed, but with higher density than has been reported for cones,^{13,14,16} and these were suspected to be rods.²⁵ The region of the relative scotoma also showed some structure consistent with retinal pigment epithelial (RPE) cells, which have been shown to be directly visible in instances where photoreceptor cells have been lost¹⁴ (Figure 2).

Two-color dark-adapted modified Goldmann kinetic perimetry²¹ and fundus-guided microperimetry were performed to assess whether the remaining visual function was rod-mediated in the region of relative scotoma. The superimposed isopters from the 2 stimuli indicated that the test was rod-mediated (Figure 3). Two-color dark-adapted modified microperimetry, as described previously, also indicated rod-mediated function (Figure 3).^{22,23}

AOSLO images were taken at 4 time points over a period of 48 months. Although the image quality of the imaging sessions differed, the cone mosaic appeared stable, and there was no evidence of progressive cone loss. SD-OCT images taken 10 months apart also indicated no change in the decreased reflectance of the IS/OS junction within the region of lesion.

• **CASE 3:** A 27-year-old myopic woman presented with acute vision loss and photopsias in the right eye, initially starting in the mid-periphery and moving to involve fixation. The peripheral visual field abnormalities improved over the next 3 months but she retained a central scotoma with discrete borders. Past medical history included autoimmune hepatitis diagnosed at age 16 and autoimmune thyroiditis. MRI of the head was normal. There were no fundus abnormalities in either eye.

within which no cones are visible. The large inset (black rectangle) highlights the retinal region of normal cone spacing transitioning into abnormal or sparse cone spacing (black circles). The smaller insets (white squares) show a transition from cones to a localized region of hexagonal cells (white arrows) in addition to a localized retinal region with tightly packed cells, suspected to be rods. The retinal region where RPE cells were observed is different from the region noted with presumed rods. The SD-OCT scan (location indicated by the green line on the background image) shows reduced reflectance of the IS/OS junction within the relative scotoma. The inset above the SD-OCT B-scan highlights the reflectance change.

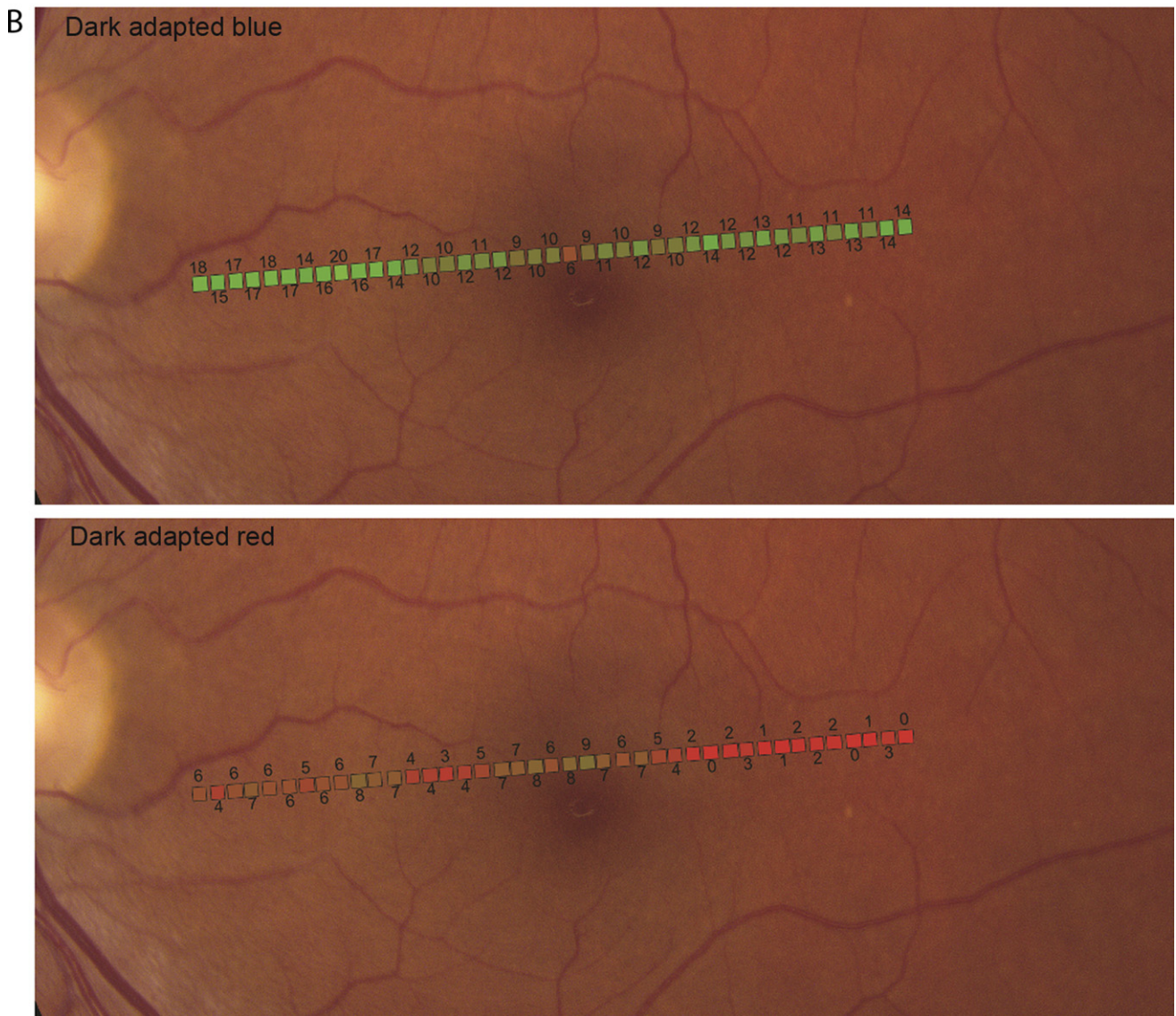
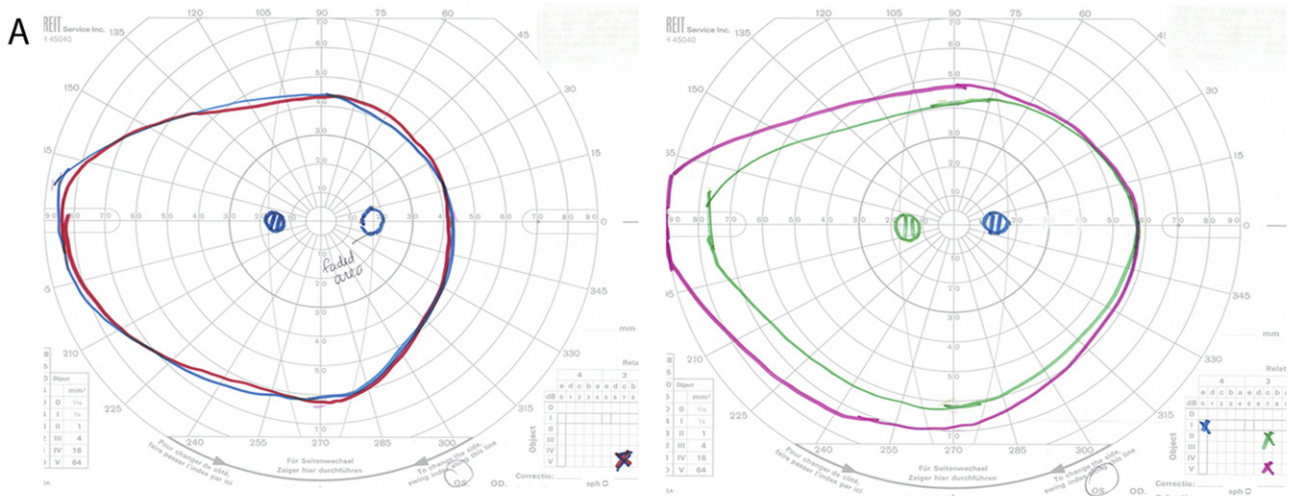


FIGURE 3. Acute zonal occult outer retinopathy. (Top) Kinetic perimetry for Patient 2, left eye. (Left) Two-color dark-adapted Goldmann kinetic field isopters. The isopter for the V₃c long-wavelength stimulus target (red solid line) and the isopter for the V₃c short-wavelength stimulus target (blue solid line) are superimposed. The isopter for the II₃c long-wavelength stimulus target and

Although the highest-density cones in the foveal center were not resolved, which is typical for eyes with normal cone packing,¹⁶ the remainder of the foveal image showed a normal cone mosaic, despite severely reduced foveal sensitivity (Figure 4).

AOSLO images taken 24 months later revealed no change in the appearance of the cones; SD-OCT was also unchanged with stable relative thinning of the inner retinal layers including the outer nuclear layer (ONL) but normal reflectance of the IS/OS, OS, and RPE layers in the affected eye.

• **CASE 4:** A 51-year-old myopic female patient presented with 4 months of reduced central vision in each eye, worse in bright light and associated with photosensitivity, and difficulty adapting from dark into light conditions.

AOSLO images of the right eye showed abnormal cone structure within the central 4 degrees from the fovea^{13,14,16} (Figure 5, right eye shown). SD-OCT images obtained 12 months later showed loss of the external limiting membrane at the fovea. Anti-retinal antibody activity involving a ~45 kd antigen was identified in a Western blot of porcine retina.²⁶⁻²⁹

DISCUSSION

THE MECHANISM OF VISION LOSS IN AZOOR PATIENTS remains uncertain, although photoreceptor, inner retinal, and RPE dysfunction has been documented.¹⁻³ To our knowledge, no histologic studies exist describing the effect of AZOOR on cone structure, but several recent reports have shown attenuation of the IS/OS junction and outer retinal loss in cross-section using both time-domain and spectral-domain OCT.^{5-8,30} We observed similar findings in 3 of our 4 patients and extended our studies to include direct en-face visualization of cone photoreceptor cells using AOSLO.

The AOSLO image in the first patient showed focal areas of reduced cone reflectivity indicated by dark patches, interspersed with regions of contiguous and normal cone spacing (Figure 1). The reduced cone reflectivity could indicate morphologic alterations that interfere with the wave-guiding properties of the cones.³¹

Despite the loss of visible cones in the AOSLO image in Patient 2, the IS/OS junction was continuous, although reflectance of this layer was reduced (Figure 2), representing a significant change in actual reflectance in the region of the relative scotoma since OCT images are displayed on a logarithmic scale. Whereas loss of cone reflectance is generally observed as disruption of the IS/OS layer (Figure 1), the presence of a visible IS/OS junction in the scotomatous area where unambiguous cones were not visible suggests cones may have been absent or very sparse in the areas of the scotoma, but that rods remained. We did not see a shift in the outer termination of the photoreceptor outer segments across the transition to the rod-only region as we might have expected based on some recent high-resolution SD-OCT studies.³² We suspect this is attributable to the poorer resolution of our commercial SD-OCT system.

In patients with dense scotomas and areas in which unambiguous cones were not visualized, mosaics of polygonal RPE cells were imaged (Figures 2 and 5). Although these images provide no information on the health of the RPE cells, they suggest that in some AZOOR patients, RPE cells persist in the absence of overlying cones.

In Patient 3 cone reflectivity, contiguity, and spacing were no different from normal, despite central visual loss (Figure 4). Photoreceptors may be initially dysfunctional but preserved in early stages of AZOOR, and lost only in later stages,⁵ but serial AOSLO images over 24 months showed no evidence of progressive photoreceptor loss in this patient. Inner retinal dysfunction as measured by delayed 30-Hz flicker implicit time has been reported in AZOOR patients³ and was present in Patient 3. The present manuscript provides images of an intact cone mosaic and outer retinal layers in a region with central vision loss and evidence of inner retinal dysfunction measured by delayed 30-Hz flicker timing, as well as thinning of the inner retinal layers, providing support for the observation that vision loss in patients diagnosed with AZOOR can be caused by inner retinal dysfunction in the presence of normal cone structure.

In Patient 4, repeated SD-OCT imaging revealed reduced outer retinal thickness over 1 year (Figure 5), consistent with reports that AZOOR may progress in 4% of patients.¹ The patient with a history of autoimmune

the isopter for the II $\bar{3}$ c short-wavelength stimulus target (not shown) were also superimposed. In these rod-mediated tests, the scotoma is absent and both red and blue stimuli were seen as achromatic, although the patient reported the blue targets to appear "blurry or dimmer" in the region of the scotoma. (Right) Light-adapted Goldmann kinetic field isopters obtained by using a white target stimulus shows full peripheral fields with the II $\bar{3}$ c and V $\bar{3}$ c targets; the I4e stimulus shows the scotoma. (Bottom) Dark-adapted 2-color fundus-guided microperimetry for Patient 2, left eye. The data from microperimetry are superimposed onto a fundus image. (Top) Dark-adapted blue (Blue DA) sensitivities were normal throughout the regions tested (background illuminance of 0 cd/m², 200 ms Goldmann V blue stimulus, 2.0 neutral density [ND] filter). (Bottom) Dark-adapted red (Red DA) sensitivities showed a dense scotoma beginning about 3 degrees temporal to fixation (background illuminance of 0 cd/m², 200 ms Goldmann V red stimulus, 1.0 ND filter). The difference between Blue DA and Red DA sensitivity values for each retinal location in the region of scotoma was at least 8 dB, demonstrating rod-mediated sensitivity in the scotomatous region.

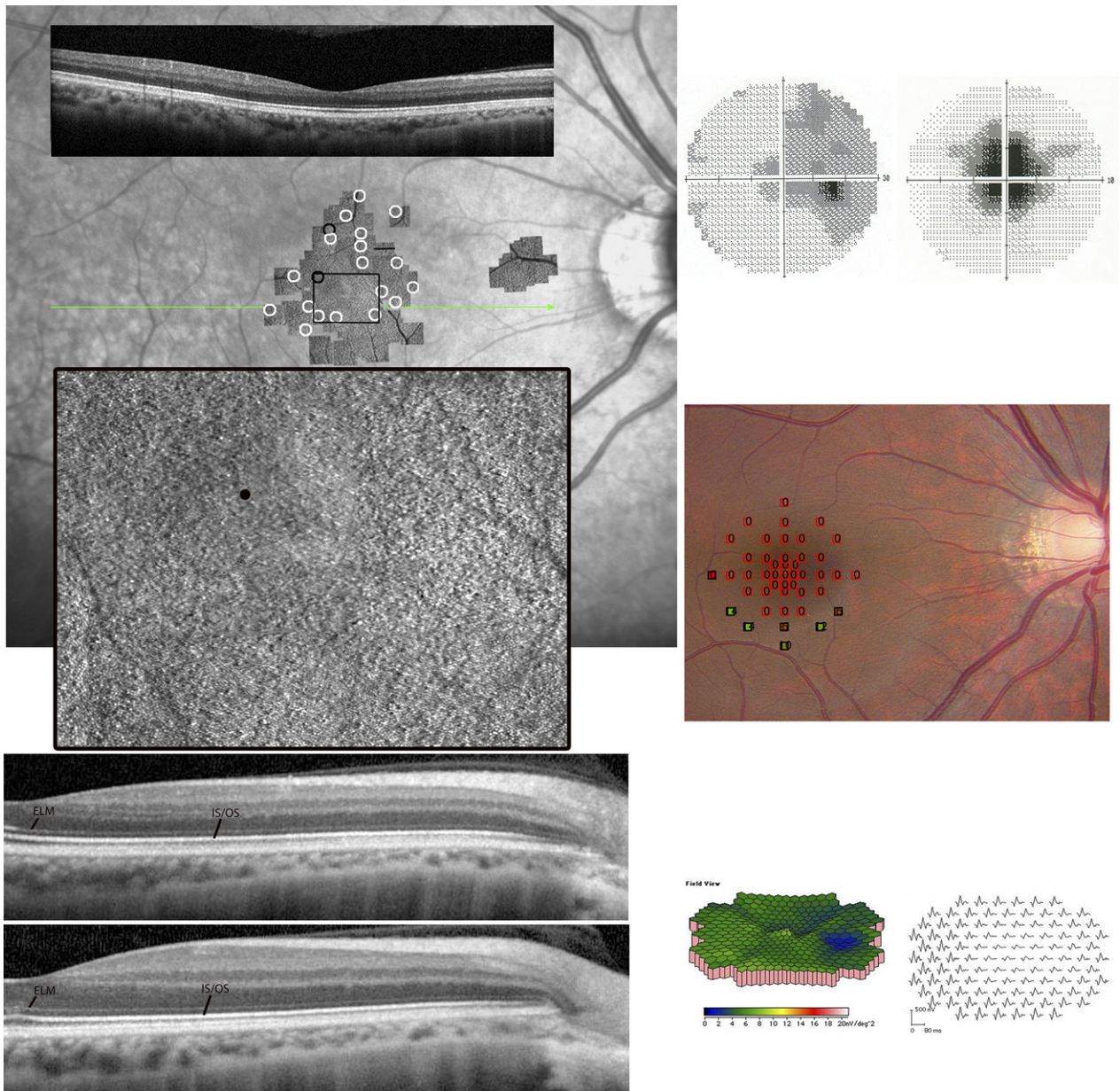


FIGURE 4. Acute zonal occult outer retinopathy, Patient 3, right eye. (Top left) The composite AOSLO image superimposed on an infrared fundus image reveals normal cone spacing and coverage (white circles) throughout the macula in the affected right eye despite the central scotoma. Two retinal locations indicated slightly abnormal cone spacing (black circles) but an otherwise contiguous cone mosaic. The composite image spans approximately 6.6×8.25 degrees (scale bar is 1 degree). The smaller AOSLO montage toward the disc indicates the location of the preferred retinal locus for fixation. (Center left) The magnified AOSLO montage is indicated by the black inset. The black dot in the inset is the location of the anatomic fovea. The SD-OCT scan (green line indicates scan location) shows an uninterrupted IS/OS junction layer corresponding to the central region of scotoma. (Bottom left) SD-OCT scans of the affected right eye (top) and the normal left eye (bottom). The left eye has been flipped horizontally for comparison purposes. ELM and IS/OS junction layers are labeled. The symptomatic eye shows attenuation of the outer nuclear and inner retinal layers compared to the contralateral eye. The laminar appearance of the optical components of the photoreceptors shows normal reflectance of the IS/OS junction across the macula, with subtle abnormalities of the OS/RPE junction. (Top right) Humphrey visual field (HVF) 30-2 at presentation (left) and 10-2 3 months later (right) reveals the initial temporal visual field defect decreasing in size, resulting in a central scotoma 6 degrees in diameter over 3 months, which persisted 2 years after symptoms onset; foveal sensitivity was reduced by at least 3.5 log units. (Center right) The data from microperimetry is superimposed onto the fundus image. Microperimetry using a white background and a white Goldmann III 200 ms stimulus reveals at least 2 log units sensitivity loss in the central 4 degrees in diameter. (Bottom right) The mfERG first-order responses displayed in field view also reveal unilateral reduced response densities centrally corresponding with the HVF defect.

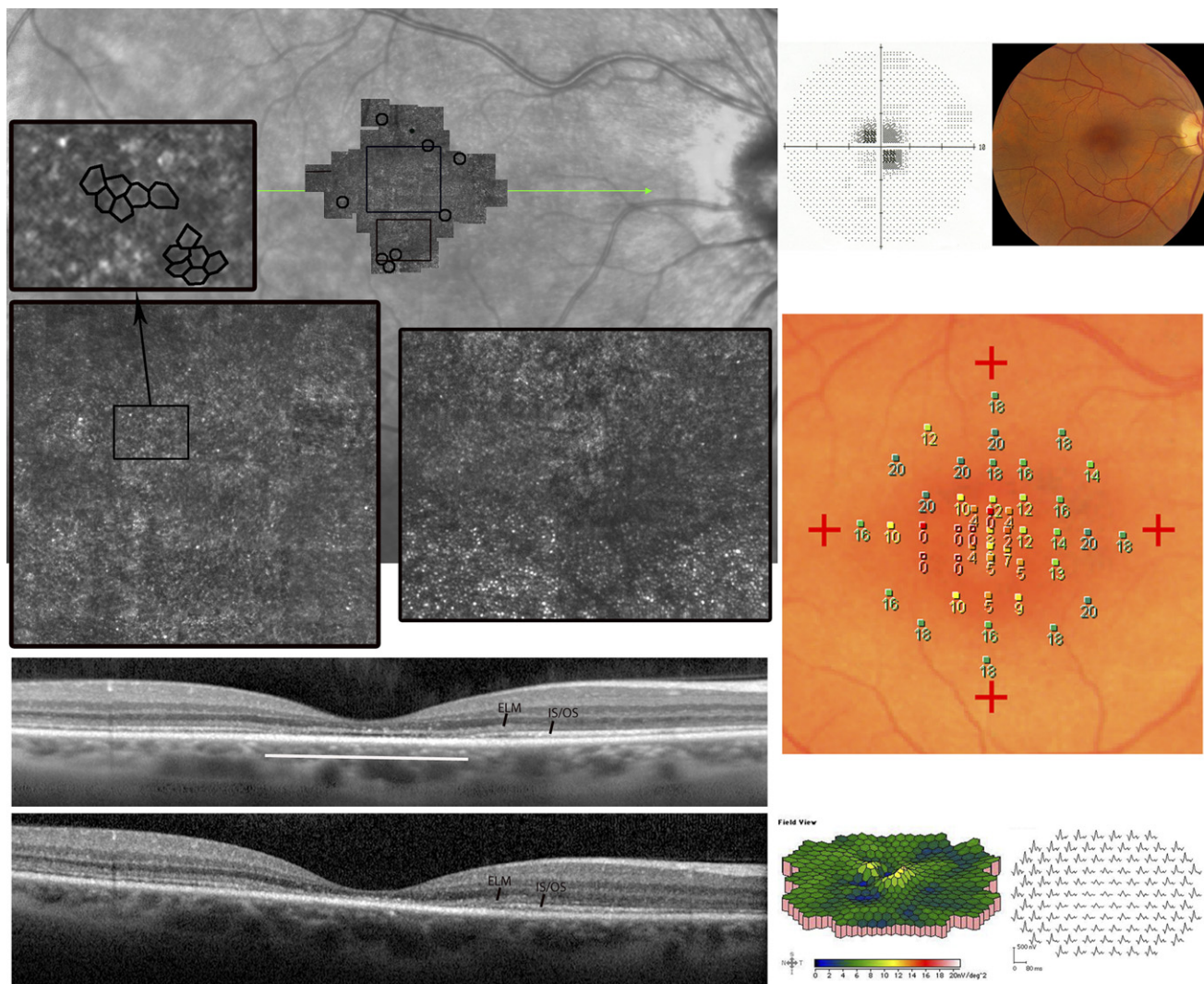


FIGURE 5. Acute zonal occult outer retinopathy, Patient 4, right eye. (Top left) The composite AOSLO image, which spans approximately 7.7×7 degrees (scale bar is 1 degree), is superimposed on an infrared (IR) SLO fundus image. The AOSLO image shows a region of abnormal cone structure within the macula. The preferred retinal locus for fixation is superior to the anatomic fovea and is labeled with a small black circle. Cones at the edges of the AOSLO field have lower density than normal (black circles). The locations of the insets are indicated by the black rectangles on the AOSLO montage. The lower left inset over the foveal center reveals sparse, irregularly arranged cones and hexagonal cells consistent with retinal pigment epithelial (RPE) cells. A detail of the RPE cells is shown in the upper left inset. The right inset shows the transition from absence to presence of regular cone mosaics, albeit with reduced density. The SD-OCT scan (location indicated by green line on the IR fundus image) indicates disruption and loss of the inner/outer segment (IS/OS) junction in the central macula along with thinning of the outer nuclear layer. (Bottom left) SD-OCT 12 months after initial presentation shows further loss of the IS/OS junction and outer segment layer, indicating progressive loss of the optical components of the photoreceptors in the macula. External limiting membrane (ELM) and inner/outer segment junction layers (IS/OS) are labeled. (Top right) Reduced visual acuity of 20/200 corresponds to a 4-degree-diameter central scotoma with reduced foveal sensitivity of 18 dB (normal >34 dB). (Top right) RPE depigmentation is present in the fovea. (Center right) Fundus-guided microperimetry using a white background and a white Goldmann III 200 ms stimulus shows reduced sensitivities by 1 to 2 log units in the central 2 degrees. Similar results were observed in the left eye (not shown). (Bottom right) Multifocal electroretinographic first-order response densities are reduced in the central 5 to 10 degrees.

disease (Patient 3) showed no abnormal anti-retinal antibody activity. The 45 kd reaction in the fourth patient represents the first report of potentially clinically significant anti-retinal antibody activity in a patient with AZOOR, and may support the hypothesis that autoimmune reactions against retinal cells may, in some cases,

contribute to or occur in response to the development of AZOOR.

In conclusion, we have used AOSLO to image AZOOR patients, providing high-resolution montages of the central retina. Adaptive optics provide a sensitive measure of macular cone structure in normal subjects,¹⁶ and in

AZoor patients AOSLO was used to demonstrate photoreceptor structure in regions of vision loss that were manifested as a normal mosaic of cones, regions of cone loss, and alteration in cone structure. This study is the first

to measure in vivo cone spacing and to image rods in AZoor patients. We report retinal heterogeneity in subjects diagnosed with AZoor based on direct visualization of photoreceptors in living retina.

ALL AUTHORS HAVE COMPLETED AND SUBMITTED THE ICMJE FORM FOR DISCLOSURE OF POTENTIAL CONFLICTS OF Interest. Publication of this article was supported by Foundation Fighting Blindness, Columbia, Maryland; Research to Prevent Blindness, New York, New York; Hope for Vision, Washington, D.C.; That Man May See, Inc., San Francisco, California; and National Institute of Health, (Bethesda, Maryland) grants EY014375, EY002162, 1 P30 EY12576-6, NIH K12 EY017269, NIH T35 EY007139-16.. Austin Roorda holds a patent (US Patent # 7118216) for adaptive optics scanning laser ophthalmoscopy technology. Brandon Lujan is a consultant for Carl Zeiss Meditec, AG and Genentech, Inc. Involved in design and conduct of the study (A.R., B.L., J.L.D.); collection, management, analysis, and interpretation of the data (M.M., B.J.L., D.M., C.E.T., A.R., J.L.D.); and preparation, review, and approval of the manuscript (M.M., B.L.J., C.E.T., A.R., J.L.D.). Research procedures adhered to the tenets of the Declaration of Helsinki. The study protocol was approved prospectively by the institutional review boards of the University of California, San Francisco; the University of California, Berkeley; and the University of California, Davis. All subjects gave written informed consent before participation in the studies, and the work was HIPAA-compliant. The trial was registered on www.clinicaltrials.gov as NCT00254605. The authors thank David Birch, Retina Foundation of the Southwest, Dallas, Texas for guidance on dark- and light-adapted 2-color microperimetry protocol development. The authors also thank Carl Jacobsen, UC Berkeley School of Optometry, Berkeley, California for sharing his clinical findings on Patient 3.

REFERENCES

1. Gass JD, Agarwal A, Scott IU. Acute zonal occult outer retinopathy: a long-term follow-up study. *Am J Ophthalmol* 2002;134(3):329–339.
2. Jacobson SG, Morales DS, Sun XK, et al. Pattern of retinal dysfunction in acute zonal occult outer retinopathy. *Ophthalmology* 1995;102(8):1187–1198.
3. Francis PJ, Marinescu A, Fitzke FW, Bird AC, Holder GE. Acute zonal occult outer retinopathy: towards a set of diagnostic criteria. *Br J Ophthalmol* 2005;89(1):70–73.
4. Jampol LM, Becker KG. White spot syndromes of the retina: a hypothesis based on the common genetic hypothesis of autoimmune/inflammatory disease. *Am J Ophthalmol* 2003;135(3):376–379.
5. Zibrandtsen N, Munch IC, Klemp K, Jorgensen TM, Sander B, Larsen M. Photoreceptor atrophy in acute zonal occult outer retinopathy. *Acta Ophthalmol* 2008;86(8):913–916.
6. Li D, Kishi S. Loss of photoreceptor outer segment in acute zonal occult outer retinopathy. *Arch Ophthalmol* 2007;125(9):1194–1200.
7. Spaide RF, Koizumi H, Freund KB. Photoreceptor outer segment abnormalities as a cause of blind spot enlargement in acute zonal occult outer retinopathy-complex diseases. *Am J Ophthalmol* 2008;146(1):111–120.
8. Fujiwara T, Imamura Y, Giovannozzo VJ, Spaide RF. Fundus autofluorescence and optical coherence tomographic findings in acute zonal occult outer retinopathy. *Retina* 2010;30(8):1206–1216.
9. Liang J, Williams DR, Miller DT. Supernormal vision and high-resolution retinal imaging through adaptive optics. *J Opt Soc Am A Opt Image Sci Vis* 1997;14(11):2884–2892.
10. Roorda A, Romero-Borja F, Donnelly W III, Queener H, Hebert T, Campbell M. Adaptive optics scanning laser ophthalmoscopy. *Opt Express* 2002;10(9):405–412.
11. Carroll J, Neitz M, Hofer H, Neitz J, Williams DR. Functional photoreceptor loss revealed with adaptive optics: an alternate cause of color blindness. *Proc Natl Acad Sci U S A* 2004;101(22):8461–8466.
12. Choi SS, Doble N, Hardy JL, et al. In vivo imaging of the photoreceptor mosaic in retinal dystrophies and correlations with visual function. *Invest Ophthalmol Vis Sci* 2006;47(5):2080–2092.
13. Duncan JL, Zhang Y, Gandhi J, et al. High-resolution imaging with adaptive optics in patients with inherited retinal degeneration. *Invest Ophthalmol Vis Sci* 2007;48(7):3283–3291.
14. Roorda A, Zhang Y, Duncan JL. High-resolution in vivo imaging of the RPE mosaic in eyes with retinal disease. *Invest Ophthalmol Vis Sci* 2007;48(5):2297–2303.
15. Wolfing JI, Chung M, Carroll J, Roorda A, Williams DR. High-resolution retinal imaging of cone-rod dystrophy. *Ophthalmology* 2006;113(6):1014–1019.
16. Yoon MK, Roorda A, Zhang Y, et al. Adaptive optics scanning laser ophthalmoscopy images in a family with the mitochondrial DNA T8993C mutation. *Invest Ophthalmol Vis Sci* 2009;50(4):1838–1847.
17. Talcott KE, Ratnam K, Sundquist SM, et al. Longitudinal study of cone photoreceptors during retinal degeneration and in response to ciliary neurotrophic factor treatment. *Invest Ophthalmol Vis Sci* 2011;52(5):2219–2226.
18. Duncan JL, Talcott KE, Ratnam K, et al. Cone structure in retinal degeneration caused by mutations in the peripherin/RDS gene. *Invest Ophthalmol Vis Sci* 2011;52(3):1557–1566.
19. Marmor MF, Holder GE, Seeliger MW, Yamamoto S; International Society for Clinical Electrophysiology of Vision. Standard for clinical electroretinography (2004 update). *Doc Ophthalmol* 2004;108(2):107–114.
20. Marmor MF, Hood DC, Keating D, et al. Guidelines for basic multifocal electroretinography (mfERG). *Doc Ophthalmol* 2003;106(2):105–115.
21. Rotenstreich Y, Fishman GA, Lindeman M, Alexander KR. The application of chromatic dark-adapted kinetic perimetry to retinal diseases. *Ophthalmology* 2004;111(6):1222–1227.
22. Jacobson SG, Voigt WJ, Parel JM, et al. Automated light- and dark-adapted perimetry for evaluating retinitis pigmentosa. *Ophthalmology* 1986;93(12):1604–1611.
23. Crossland MD, Luong VA, Rubin GS, Fitzke FW. Retinal specific measurement of dark-adapted visual function: validation of a modified microperimeter. *BMC Ophthalmol* 2011;11:5.
24. Rodieck RW. The density recovery profile: a method for the analysis of points in the plane applicable to retinal studies. *Vis Neurosci* 1991;6(2):95–111.

25. Curcio CA, Sloan KR, Kalina RE, Hendrickson AE. Human photoreceptor topography. *J Comp Neurol* 1990;292(4):497–523.
26. de Smet MD, Bitar G, Mainigi S, Nussenblatt RB. Human S-antigen determinant recognition in uveitis. *Invest Ophthalmol Vis Sci* 2001;42(13):3233–3238.
27. Yoon YH, Cho EH, Sohn J, Thirkill CE. An unusual type of cancer-associated retinopathy in a patient with ovarian cancer. *Korean J Ophthalmol* 1999;13(1):43–48.
28. Forooghian F, Macdonald IM, Heckenlively JR, et al. The need for standardization of antiretinal antibody detection and measurement. *Am J Ophthalmol* 2008;146(4):489–495.
29. Adamus G, Wilson DJ. The need for standardization of antiretinal antibody detection and measurement. *Am J Ophthalmol* 2009;147(3):557
30. Fine HF, Spaide RF, Ryan EH Jr, Matsumoto Y, Yannuzzi LA. Acute zonal occult outer retinopathy in patients with multiple evanescent white dot syndrome. *Arch Ophthalmol* 2009;127(1):66–70.
31. Roorda A, Williams DR. Optical fiber properties of individual human cones. *J Vis* 2002;2(5):404–412.
32. Srinivasan VJ, Monson BK, Wojtkowski M, et al. Characterization of outer retinal morphology with high-speed, ultrahigh-resolution optical coherence tomography. *Invest Ophthalmol Vis Sci* 2008;49(4):1571–1579.



Biosketch

Marianna Mkrtyan, OD, practices at Kagan Institute in Los Angeles, California. She received a BS with departmental honors in molecular, cell, and developmental biology from University of California, Los Angeles in 2004, and an OD from University of California, Berkeley with clinic and research honors in 2011. Before entering graduate school, she worked at UCLA studying stem cells in *Drosophila* and co-authored article publications in *Nature* and in *Developmental Genes Evolution*. Her interests are in clinical research.